Available online at www.sciencedirect.com
SCIENCE DIRECT
Catalysis Today 116 (2006) 6–11
CATALYSIS TODAY
www.elsevier.com/locate/cattod

Synthesis of nanostructured catalysts by laser pyrolysis

H. Maskrot [a], Y. Leconte [a], N. Herlin-Boime [a,*], C. Reynaud [a], E. Guelou [b], L. Pinard [b], S. Valange [b], J. Barrault [b], M. Gervais [c]

[a] *Service des Photons, Atomes et Molécules, Laboratoire Francis Perrin (CEA-CNRS URA 2453), CEA Saclay, 91191 Gif/Yvettte Cedex, France*
[b] *LACCO-ESIP (UMR CNRS 6503), 40 avenue du recteur Pineau, 86022 Poitiers, France*
[c] *(LEMA) Laboratoire d'Electrodynamique des Matériaux Avancés (UMR 6157CNRS-CEA), Tours, France*

Available online 26 May 2006

Abstract

Laser pyrolysis is a promising and versatile method allowing the synthesis of various nanoparticles, with well defined chemical composition, size and structure. This procedure is based on the interaction of a powerful IR laser beam with a mixture of gaseous or liquid precursors, with one of them absorbing the laser radiation. This paper presents the synthesis of nanoPt/TiO_2 and nanoPd/TiO_2 by laser pyrolysis and preliminary results about their efficiency for elimination of volatile organic compounds (deVOC). The nanoparticles have been synthesized by adding a metallic precursor in a liquid precursor (titanium isopropoxide). X-ray diffraction, transmission electron microscopy, thermogravimetric analysis and IR spectroscopy have been used to analyse their nanostructures and morphologies.

The volatile organic compounds elimination (deVOC) tests performed on these nanomaterials demonstrate that Pd-catalysts are very efficient in the total elimination of chloro-compounds. These catalytic properties are unusual, especially because conventional Pd supported catalysts are generally not used for this application due to a production of a high amount of polychlorinated compounds.

These results showed that the laser pyrolysis method allows the synthesis of well dispersed titanium-based catalysts not previously reported in the literature.

Keywords: Laser pyrolysis; TiO_2; Pt-TiO_2 and Pd-TiO_2

1. Introduction

Among the wide range of applications of nanomaterials (microelectronics, electromagnetism, optoelectronic, etc.), catalysis is a privileged domain of application in nanoscience. Indeed, due to the high surface of the nanostructured materials and efficient dispersion of the active phase (oxide, metal) an improvement of catalytic properties as well as the durability of the solids can be expected. In particular in the field of environmental catalysis, i.e. new processes for green chemistry, the emission of volatile organic compounds (VOC) is considered as an important environmental problem. More efficient catalytic materials and processes are needed to eliminate VOC from various effluents and nanoparticles containing a well dispersed active phase appear to be good candidates to achieve this objective. The laser pyrolysis method is a powerful and versatile method to produce such nanoparticles with well defined chemical composition, size and structure [1–3] and a high specific surface. This method is based on the interaction of a powerful infrared (IR) laser beam with a mixture of gaseous or liquid precursors, one of them absorbing the laser radiation. In the interaction zone, the absorption of laser radiation leads to a fast increase of temperature, precursors are decomposed and an incandescent flame where nanoparticles nucleate and grow can be observed. The characteristics of the nanoparticles are strongly correlated with the experimental parameters; in particular the size of the nanoparticles depends on the residence time in the laser beam adjusted by the gas flow rates of reactants. Their chemical composition depends on the nature and the content of the different reagents in the precursor mixture.

Materials traditionally used for the decomposition of VOC are noble metals supported on oxide phases. This paper deals with Pt and Pd supported on TiO_2 nanoparticles. Pure TiO_2

* Corresponding author. Tel.: +33 1 69 08 36 84; fax: +33 1 69 08 87 07.
E-mail address: nathalie.herlin@cea.fr (N. Herlin-Boime).

0920-5861/$ – see front matter © 2006 Elsevier B.V. All rights reserved.
doi:10.1016/j.cattod.2006.04.006

nanopowders have already been obtained by laser pyrolysis from various liquid precursors such as: titanium isopropoxide (TTIP), $Ti(OC_3H_7)_4$ [4,5] or titanium ethoxide $Ti(OC_2H_5)_4$ [4]. Doped TiO_2 nanopowders (Mo, W, Al, Ga) were also prepared by laser pyrolysis from TTIP precursor [6,7]. In this study, Pt and Pd supported on TiO_2 nanoparticles have been synthesized by laser pyrolysis and characterized from a structural point of view. The evolution of experimental parameters (laser power, composition of the precursor phase, etc.) is correlated with structural organization of the powders. Moreover, first tests of catalytic activity for destruction of methanol and chlorobenzene of the laser-synthesized catalysts are presented. The results are compared with standard catalyst and impregnated nanoTiO_2 and reveal a promising behaviour of the laser synthesized nanopowders.

2. Experimental

2.1. Pt– and Pd–TiO_2 preparation

2.1.1. Laser pyrolysis

The Pt–TiO_2 and Pd–TiO_2 nanopowders were synthesized by laser pyrolysis using TTIP as Ti precursor. The solutions containing the precursors were prepared by first dissolving appropriate amounts of palladium acetylacetonate Pd(Acac) (Aldrich 97% purity) or platinum acetylacetonate Pt(Acac) (Aldrich, 97% purity) in different solvents. For Pt–TiO_2 nanopowders, absolute ethanol or a xylene (Aldrich, 98% purity)/ethylacetate (SDS, purum) mixture (65:35, v/v) were used; the latter procedure was already described by Strobel [8]. The obtained solutions were then mixed with TTIP (Aldrich, 97%). Nevertheless, such solutions absorb only weakly the laser radiation and ethylene C_2H_4 was added as sensitizer gas. The aerosol was produced by an ultrasonic spraying generator (Pyrosol model, RBI) which has been widely used in thin films deposition. In the experiments reported here, aerosol droplets were carried out in a flow of neutral gas into the reaction chamber through a 6 mm diameter nozzle. This flow which controls the amount of mixture introduced in the reactor was fixed at 2000 $cm^3\ min^{-1}$ and allows to carry about 45–50 g of reactants per hour in the reaction chamber. A flow of co-axial argon allows confining the reaction in a very small volume without any interaction with reactor walls and was fixed to 2200 $cm^3\ min^{-1}$. Ethylene gas and aerosol were mixed just before the reaction zone and this flow of reactants intersects orthogonally the laser beam which can be focused using a cylinder lens (plane of the beam is orthogonal with the axis of the nozzle). The pressure was maintained constant at the atmospheric value through a regulated pumping system and the powders were collected on filters placed downstream from the reaction zone. Table 1 presents the main experimental parameters involved in the different synthesis reported here.

2.1.2. Chemical impregnation

The Pt/SiO_2 reference solid used for catalytic tests was prepared through a classical impregnation of a commercial silica (Aerosil D200, Degussa) with an aqueous solution of diaminodinitroplatinum(II) $[Pt(NH_3)_2(NO_2)_2]$. After impregnation, the solid was left to evaporate and dried at 100 °C in an oven, before annealing in air flow at 450 °C for 4 h.

2.2. Characterization methods

The obtained powders were characterized as-formed and after heat treatments under air. The heat treatments were carried out in an oven (PYROX HE60/16). The heating rate was 5 °C min^{-1} and the dwell time 3 h. Chemical analyses were performed using conventional methods (CNRS analytical center/Solaize-France) with a relative uncertainty of ±2% for C, O, and of ±3% for Pt, Pd and Ti determination. Information about the chemical bonding was obtained by Fourier transform infra-red (FT-IR) spectrophotometry (Perkin-Elmer 2000 FT-IR spectrophotometer) in the 4000–400 cm^{-1} range using the KBr pellet technique. The specific surface areas (S_{BET}) were measured by the BET method using a Micromeritics Flowsorb 2300. The powder density (ρ) was measured by Helium pycnometry (Micromeritics AccuPyc 1330). An equivalent diameter (D) was estimated from D and ρ by using the well known expression: $D = 6/\rho$. S_{BET} and assuming a spherical shape for the particles.

X-ray diffraction (XRD) powder patterns were obtained with an automated diffractometer (Philips, APD1700) using the Cu Kα radiation. To study the morphology and the surface of Pt–TiO_2 particles as well as the Pt particle size, a TEM (Philips CM120 microscope, equipped with a LaB6 filament at 120 kV) coupled to an EDX analyser (fixed probe) analysis was used.

Table 1
Main experimental parameters and characterization results

Powder	Power laser (W)	Focalized	Solvent	M:TiO_2 ratio solution	M:TiO_2 ratio (wt.%)	Weight lost after annealing (400 °C/3 h)
Pt01/TiO_2	650	No	Xylene/ethylacetate	0.5	0.54	5
Pt02/TiO_2	990	Yes	Ethanol absolute	0.05	0.044	5
Pt03/TiO_2	990	Yes	Ethanol absolute	0.15	0.11	3.6
Pt04/TiO_2	990	Yes	Ethanol absolute	0.3	0.13	3.5
Pt05/TiO_2	990	Yes	Ethanol absolute	0.5	0.31	3.5
Pt06/TiO_2	990	Yes	Xylene/ethylacetate	0.5	0.47	10
Pt07/TiO_2	650	Yes	Xylene/ethylacetate	0.5	0.42	4
Pd/TiO_2	650	No	Xylene/ethylacetate	0.5	0.36	n.m.

M = metal.

Electron microdiffraction patterns were also recorded to identify the nature of the platinum-bearing particles. The samples were at first occluded in a resin that was cut into sections of 30–50 nm with a microtome equipped with a diamond cutter, before they were supported on a carbon-coated nickel grid. To measure the amount of accessible metal, H_2-chemisorption was performed by using a Micromeritics AutoChem 2910 instrument. The sample was first reduced under H_2 at 450 °C during 8 h, and then purged by an Ar flow for 6 h at 450 °C. H_2-chemisorption was performed using a dynamic pulse method at ambient temperature with a loop gas of 5% H_2–Ar until the integrated areas of consecutive pulses were constant.

2.3. Catalytic tests

In order to provide highly reproducible results, such studies requires the use of an isothermal flow reactor able to work semi-automatically. In all cases, to avoid effect of carbon which can evolve during catalytic reaction, the samples were annealed before the catalytic tests.

2.3.1. Methanol oxidation

The gaseous mixture used for the reaction of methanol oxidation [9] consisted of oxygen and methanol vapor, diluted by helium. The methanol flow rate was managed by using a 'saturator', containing a hot (60–80 °C) methanol solution through which the O_2–He mixture was bubbling. The final composition of the feed is controlled by the methanol partial pressure by means of a condenser in which the temperature of the circulating cooling fluid was fixed by a cryostat at 11 °C. The catalytic reactor consists of a straight Pyrex glass tube where the catalyst is held by two quartz wool plugs.

A sample loop connected to a 10-port valve allows to inject into a gas chromatograph (GC) either a known volume of the gas mixture from the reactor, or the reactant feed (by-pass position). The sample loops are connected so as to inject into the GC analyzer (involving a column packed with chromosorb 107) a known volume (0.5 ml for the FID), either of the reactant feed or of the gas mixture. A computerized system was used for the acquisition and treatment of the chromatograms. The apparatus allowed the accurate measurement of the surface area of the formaldehyde peak down to a value corresponding to a yield of 0.5%, for an initial methanol concentration of 7.7%.

2.3.2. Catalytic oxidation of chlorobenzene

Catalytic activity tests were carried out in a fixed bed reactor (i.d. = 5 mm), at atmospheric pressure in the 250–350 °C range using 0.10 g of catalyst (grain size between 200 and 400 μm). Before reaction, catalyst samples were pre-treated in situ under hydrogen airflow (60 ml min^{-1}) at 400 °C for 12 h, then cooled down to the reaction temperature 350 °C. C_6H_5Cl was introduced into the reactor using a bubbling flask containing C_6H_5Cl swept by a dry airflow, leading to a gaseous mixture directed to a condenser maintained at −16 °C. The resulting effluent was mixed with wet air to ensure that hydrometric level was matching industrial conditions. For standard conditions, the reactant mixture contained 1.03% of water (corresponding to an hydrometric of about 50%) and 667 ppm of C_6H_5Cl. The total gas flow was 90 ml min^{-1} with a GHSV of 55 000 h^{-1}. The reaction products were analysed using an on-line gas chromatograph, equipped with a FID detector and a column for the analysis of C_6H_5Cl and $PhCl_2$+ and with a FID coupled with methanisor and a column for CO_2 and CO analysis. The carbon balance, including the amount of carbon deposited on the catalyst at the end of reaction, was always higher than 95%.

3. Results and discussion

During the synthesis experiment, a well-defined orange flame is observed in the reaction zone. Due to low density of the flame, the optical pyrometer could not deliver a reliable temperature measurement. However, from naked eye observations through a glass window, it is clear that the temperature and the height of flame increase when laser power increases. The brightness of the flame is related to the flame temperature. In our case, an increase of brightness is induced by an increase of temperature. The production rate is always in the range 3–4 g h^{-1} which is sufficient for powder characterization and catalytic tests, the production range could be increased by increasing the amount of precursors carried to the reaction zone and improving the dissociation efficiency.

3.1. Characterization of the powder

The main results of the nanoPt/TiO_2 nanopowders characterization (particle size and composition) are presented in Table 2. For easier comparison, the column (Pt)/(Pt–TiO_2) in

Table 2
Main structural data for TiO_2-based catalysts

Powder	M:TiO_2 ratio solution	M:TiO_2 ratio (wt.%)	S_{BET} (m^2 g^{-1})[a]	Density, ρ (g cm^{-3})[a]	Particle equivalent diameter D_{BET} (nm)
Pt01/TiO_2	0.5	0.54	92	3.7	18
Pt02/TiO_2	0.05	0.044	144	3.8	11
Pt03/TiO_2	0.15	0.11	148	3.8	11
Pt04/TiO_2	0.3	0.13	172	3.8	9
Pt05/TiO_2	0.5	0.31	169	3.8	9
Pt06/TiO_2	0.5	0.47	147	3.7	11
Pt07/TiO_2	0.5	0.42	122	3.7	13
Pd/TiO_2	0.5	0.5	66	n.m.	n.m.

n.m.: not measured.
[a] On powder heated at 400 °C/3 h.

solution already presented in Table 1 has been added in Table 2. By comparing the different samples synthesized with absolute ethanol (samples Pt02/TiO_2 to Pt05/TiO_2, see Table 1), it can be seen that increasing the metal concentration in the solution leads to an increase of the metal concentration in the powder. Nevertheless, the comparison of samples synthesized with the same metal concentration but from absolute ethanol (sample Pt05/TiO_2) or from the xylene/ethylacetate mixture (samples Pt01/TiO_2, Pt06/TiO_2 and Pt07/TiO_2) clearly shows a better incorporation of platinum when the xylene/ethylacetate mixture is used, the Pt/(Pt–TiO_2) ratio in solution and in the resulting powder are similar in this latter case. This effect is attributed to a better dissolution of platinum acetylacetonate in the xylene/ethylacetate mixture. Changing the laser power (samples Pt06/TiO_2 and Pt07/TiO_2) or focussing the laser beam (samples Pt01/TiO_2 and Pt07/TiO_2) does not seem to produce an effect on the Pt content in the powder. Table 1 also presents the weight loss of the different samples, this weight loss is attributed to the presence of free carbon in the as formed samples as confirmed by chemical analyses. After this heating treatment, the carbon is totally eliminated. Table 1 shows that the amount of carbon is mainly related to the laser power and the nature of solvent: it strongly increases when the laser power increases from 650 to 990 W (sample Pt06/TiO_2 and Pt07/TiO_2) and when ethanol is replaced by the xylene/acetate mixture (sample Pt05/TiO_2 and Pt06/TiO_2). On the contrary it does not depend on the content of platinum (sample Pt02/TiO_2 to Pt05/TiO_2). These observations support the interpretation that this free carbon is probably stemming from a partial cracking of ethylene [5] and decomposition of solvent.

The specific surface area (S_{BET}) (92 $m^2\ g^{-1}$, see Table 2) of the sample obtained with an unfocused laser beam is equivalent to that of the Pt/TiO_2 obtained by flame synthesis with quench cooling [6]. This surface is much higher for the samples obtained with a focused laser beam (from 144 to 172 $m^2\ g^{-1}$, Table 2). Table 2 also shows that density measurements of powders containing Pt have a value close to the theoretical density of anatase TiO_2 (3.9 g cm^{-3}). Using density and S_{BET}, a grain size (diameter) in the range 9–11 nm can be calculated for samples synthesized with a focused laser beam (samples Pt02/TiO_2 to Pt07/TiO_2) and 18 nm for the sample synthesized without focusing the laser beam. This difference can be correlated to a longer residence time in the laser beam in the latter case.

For Pd/TiO_2, S_{BET} is significantly lower (66 $m^2\ g^{-1}$), this low surface may be due to strong agglomeration (see next section) confirmed by TEM micrograph (Fig. 1).

From a morphological point of view, Fig. 2 presents a low magnification TEM micrograph of a typical sample containing Pt (sample Pt01/TiO_2) after annealing; it shows that the powders are arranged in a chain like manner, they have a spherical shape and narrow size dispersion. For Pt01/TiO_2 sample, the particles sizes are in the range 15–20 nm (TEM image, Fig. 2), which is in agreement with the calculated equivalent diameter. Very few aggregates of around 55 nm were observed. Higher magnification can be used to obtain images of the Pt particles. Fig. 3 presents an example of image obtained

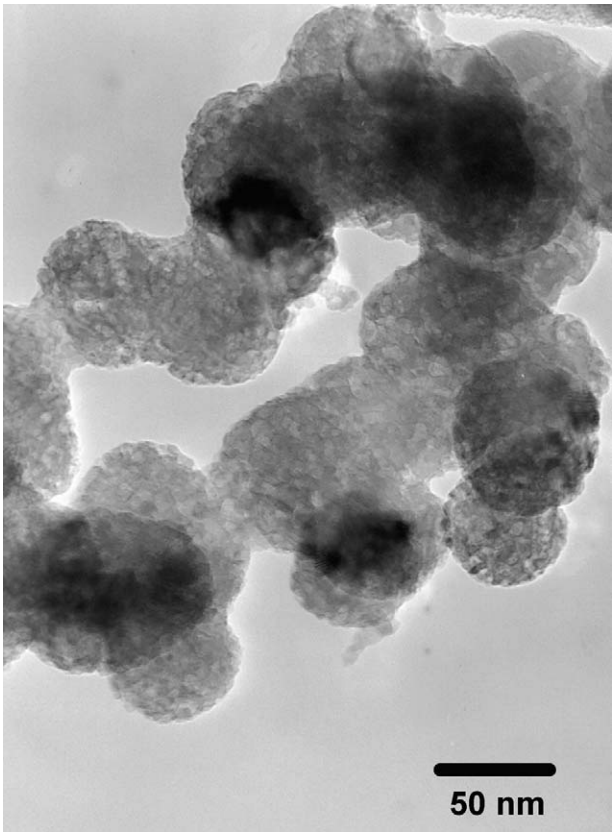

Fig. 1. TEM of the Pd/TiO_2 nanopowder after a thermal treatment at 400 °C.

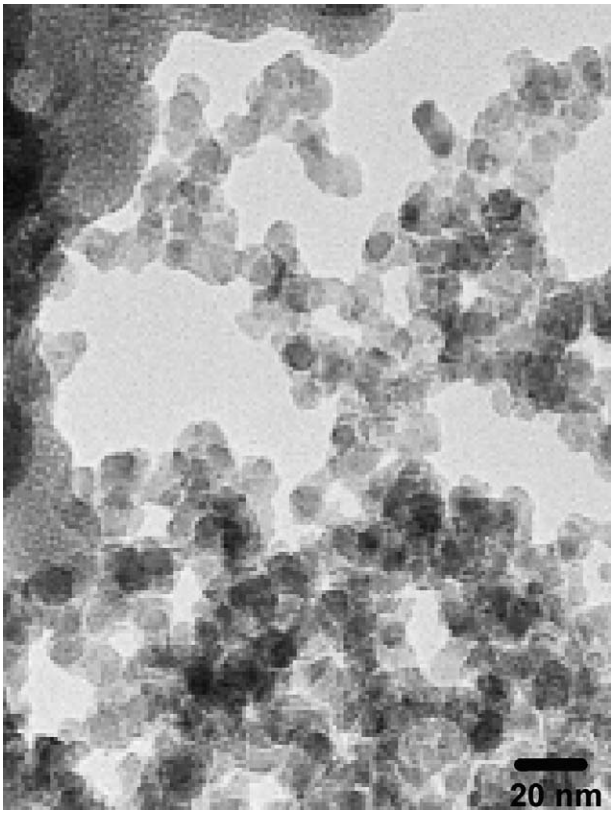

Fig. 2. TEM of a typical Pt/TiO_2 nanopowder after a thermal treatment at 400 °C (sample Pt01/TiO_2).

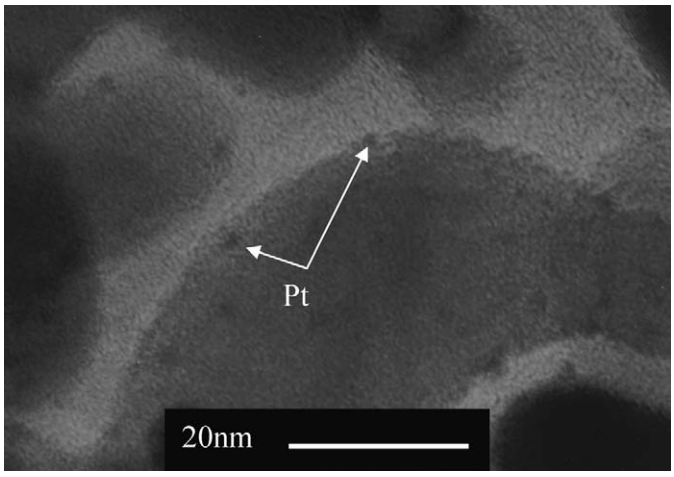

Fig. 3. TEM of the Pt–TiO_2 nanopowder, localization of Pt particles.

on the same sample (Pt01/TiO_2). It shows platinum particles of 2–3 nm in diameter, well dispersed at the surface of TiO_2. From this morphological point of view, the Pt–TiO_2 nanopowders obtained by laser pyrolysis with the laser beam ''unfocused'' appear very similar to the Pt–TiO_2 nanoparticles obtained by the flame synthesis method [12]. From H_2-chemisorption, a Pt dispersion value of 45% is obtained which indicates a mean platinum particle size of 2.6 nm, in good agreement with the value evaluated by TEM (Fig. 3).

Fig. 4 presents the FT-IR absorption spectra of annealed powders containing Pt together with a pure TiO_2 powder obtained from laser pyrolysis. The IR spectra of powders containing Pt look very similar, they mainly show the absorption bands attributed to TiO_2 superimposed on a continuous background. This background is attributed to the presence of Pt which induces a change in the electronic gap of the sample compared with pure TiO_2. At low energy, the large band corresponding to Ti–O–Ti bonding (500–700 cm^{-1}) dominates the spectra. The peaks at 3500–3150 cm^{-1} and at 1630 cm^{-1} are respectively attributed to stretching and the bending vibrations of the Ti–OH bonding [11] and appear in all

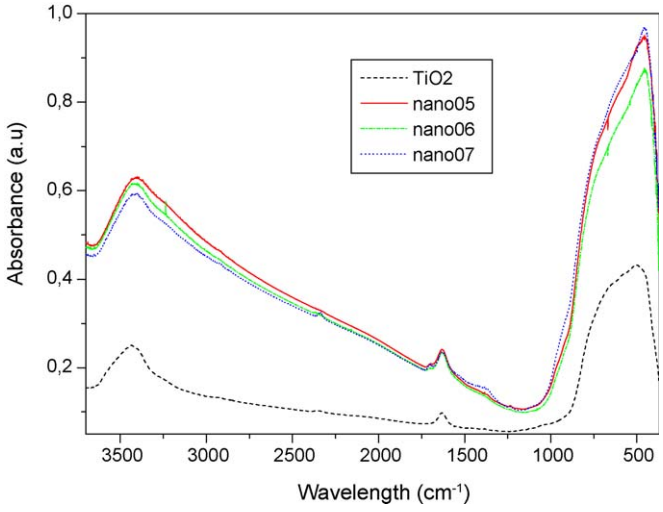

Fig. 4. FT-IR spectra of annealed sample at 400 °C during 3 h under air (samples 05, 06, 07 and pure TiO_2 laser synthesized).

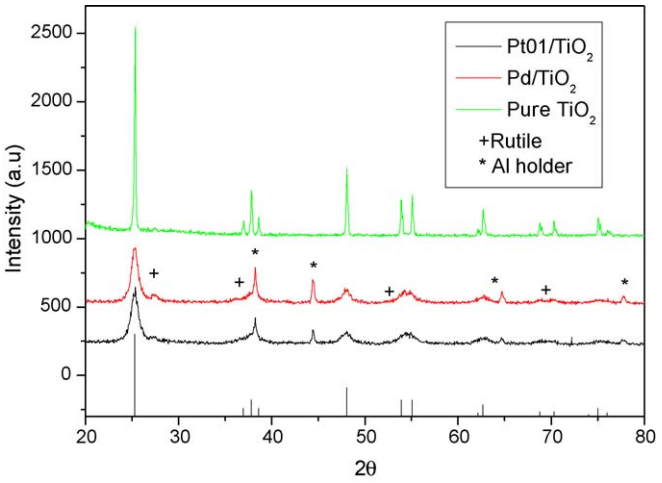

Fig. 5. XRD diagram of a typical Pt/TiO_2 (sample Pt01/TiO_2), Pd/TiO_2 and pure TiO_2 powder synthesized by laser pyrolysis (the bottom peaks correspond to the theoretical positions and intensity of the anatase phase).

the samples. The low-intensity bands at 1550–1530 cm^{-1} could correspond to the stretching vibration of Pt–O bonding [10]. The high amount of hydroxyl groups, corresponding to a low temperature form, is in good agreement with the presence of anatase which is the low temperature crystalline form identified by XRD.

The XRD patterns of Pt01/TiO_2 and Pd/TiO_2 presented in Fig. 5 correspond to a mixture of phases involving a major anatase phase and a small amount of rutile. During the synthesis of TiO_2 by laser pyrolysis, anatase is usually the only crystalline form although increasing percentages of rutile were observed at higher reaction temperature [5]. In a previous case, it has been suggested [10] that the formation of a rutile phase was promoted by the formation of PtO_2 whose structure is similar to that of rutile or that the presence of platinum favored the dehydroxylation of the sample, transforming anatase into rutile.

3.2. Catalysis: methanol oxidation

Preliminary catalytic results in methanol oxidation over Pt–TiO_2 are presented in Table 3. The ability of all the samples to

Table 3
Evaluation of the MeOH oxidation temperatures at 50% conversion over nano(Pt or Pd)/TiO_2 catalysts and comparison to a Pt/silica reference solid and impregnated TiO_2 laser synthesized

Catalyst	*M* (wt.%)	*T* (°C) at 50% methanol conversion
Pt–SiO_2 (Ref.)	0.4	115
Pt–TiO_2[a]	0.5	65
Pt01/TiO_2	0.5	80
Pt02/TiO_2	0.044	65
Pt03/TiO_2	0.11	55
Pt04/TiO_2	0.13	65
Pt05/TiO_2	0.31	55
Pt06/TiO_2	0.47	65
Pt07/TiO_2	0.42	65
Pd/TiO_2	0.36	115

[a] Impregnated TiO_2 laser synthesized.

Table 4
Conversion of chlorobenzene, selectivity into CO_2 and conversion into $PhCl_{2+}$ compounds obtained after 6 h reaction at 350 °C during oxidation of 667 ppm chlorobenzene over calcined catalysts

Catalyst	Selectivity into CO_2, X_{CO_2} (%)	Conversion of chlorobenzene, X_{PhCl} (%)	Conversion into $PhCl_{2+}$, $X_{Ph(Cl_{2+})}$ (%)
$Pt–Al_2O_3$ (Ref.)	76.5	81	3.8
Pd/TiO_2	88	99.8	3.5

favor the total elimination of methanol into CO_2 was evaluated and compared at 50% conversion.

The $Pt–TiO_2$ nanopowders synthesized by laser pyrolysis were compared with two references: a $Pt–SiO_2$ reference catalyst involving a similar Pt content (0.4 wt.% Pt) and a pure TiO_2 synthesized by laser pyrolysis was impregnated with Pt.

The catalytic results reveal that the $Pt–TiO_2$ nanopowder synthesized by laser pyrolysis and the impregnated TiO_2 laser synthesized are more active than a conventional $Pt–SiO_2$ catalyst for the complete methanol decomposition into CO_2. Indeed, the methanol oxidation over $Pt–TiO_2$ powders occurred at lower temperatures (55, 65 and 80 °C instead of 115 °C for the reference) at 50% methanol conversion (Table 3). Among the different laser synthesized samples, sample $Pt07/TiO_2$ which has the lowest specific surface and the largest diameter of particles corresponds to the less efficient catalytic results. The Pd/TiO_2 sample appears less active than Pt/TiO_2 powders for methanol conversion, probably related to the less efficient dispersion of Pd/TiO_2 sample compared to Pt/TiO_2 samples (see Figs. 1 and 2 for the general morphology). Fig. 3 illustrates the good dispersion of Pt in Pt/TiO_2 samples.

These results clearly demonstrated that the noble metals on TiO_2 nanopowders synthesized by laser pyrolysis led to very efficient catalysts in the total oxidation of methanol into CO_2. The Pt/TiO_2 nanopowders therefore lead to very efficient catalysts for the total decomposition of methanol thereby showing that the shaping of these materials could be envisaged for industrial applications.

3.3. Catalytic oxidation of chlorobenzene

The results presented in Table 4 indicate that nanoPd/TiO_2 is an active, stable and selective catalyst for the catalytic oxidation of monochlorobenzene in wet air. At 350 °C and for 667 ppm of chlorobenzene in the feed, nanoPd/TiO_2 is more active and more selective into CO_2 than a conventional catalyst such as Pt/Al_2O_3.

Table 4 shows that the pollutant conversion is 99.8% with palladium catalyst while it is only 81% with the laboratory reference. Moreover, the selectivity into CO_2 is better with the laser catalyst (88% compared to 76.5%). Therefore, these nanomaterials appeared particularly interesting for the oxidative destruction of very diluted chlorinated pollutants. Nevertheless on both catalysts the formation of polychlorinated benzenes $Ph(Cl_{2+})$ were observed and this degree of chlorination is less important in the case of Pd/TiO_2 catalyst.

4. Conclusion

Pt and Pd dispersed on TiO_2 could be obtained by laser pyrolysis which appears as a new method for synthesis of efficient catalysts. In particular, they proved to be very active and selective in the volatile organic compound elimination (MeOH and chlorobenzene) compared to conventional catalysts. This paper shows that incorporation of metal in nanopowders depends on the solvent, and the size mainly depends on the residence time. High specific surface favors efficient catalytic reaction. Further characterizations, in particular quantification of the accessibility and dispersion of the metallic phase are needed for a better comprehension of the evolution of catalytic activity.

Acknowledgements

This work was supported by the French Ministry of Economy, Finance and Industry (MINEFI) under the NACACOMO consortium.

References

[1] W.R. Cannon, S.C. Danforth, J.S. Haggerty, R.A. Marra, J. Am. Ceram. Soc. 65 (1986) 324–330.
[2] M. Cauchetier, O. Croix, N. Herlin, M. Luce, J. Am. Ceram. Soc. 77 (1994) 993–998.
[3] N. Herlin, X. Armand, E. Musset, H. Martinengo, M. Luce, M. Cauchetier, J. Eur. Ceram. Soc. 16 (1996) 1063–1073.
[4] J.D. Casey, J.S. Haggerty, J. Mater. Sci. 22 (1987) 4307–4312.
[5] F. Curcio, M. Musci, N. Notaro, G. De Michele, Appl. Surf. Sci. 46 (1990) 225–229.
[6] F. Bregani, C. Casale, L.E. Depero, I. Natali-Sora, D. Robba, L. Sangaletti, G.P. Toledo, Sens. Actuators B 31 (1996) 25–28.
[7] L.E. Depero, A. Marino, B. Allieri, E. Bontempi, L. Sangaletti, C. Casale, M. Notaro, J. Mater. Res. 15 (2000) 2080–2086.
[8] R. Strobel, W.J. Stark, L. Mädler, S.E. Pratsinis, A. Baiker, J. Catal. 213 (2003) 296–304.
[9] J.M. Tatibouet, Appl. Catal. A. 148 (1997) 213–252.
[10] T. Lopez, A. Romero, R. Gomez, J. Non-Cryst. Solids 127 (1991) 105–113.
[11] E. Sanchez, T. Lopez, R. Gomez, Bokhimi, A. Morales, NovaroF O., J. Solid State Chem. 122 (1996) 309–314.
[12] T. Johannessen, S. Koutsopoulos, J. Catal. 205 (2002) 404–408.